NUMERICAL COMPUTATION ON A SINGULARITY IN FRACTURE

B. Zhu* and Y. Chen**

*University of Science and Technology of China, Anhui, People's Republic of China
**Department of Mechanics and Materials Science, Rutgers, The State University of New Jersey, P.O. Box 909, Piscataway, N.J. 08854, USA

ABSTRACT

This paper discusses three finite element approaches in solving a two-dimensional linear elasto-static problem with fixed boundary conditions and derivative singularity $O(r^{\lambda-1})$ near a corner ($0<\mathrm{Re}\lambda<1$). This singularity occurs in the stress analysis of a layered medium under compressive load. The first approach uses the regular bilinear isoparametric quadrilateral element (Zienkiewicz, 1977). The second uses Akin's special four-node quadrilateral element (Akin, 1976) and the third is based on a generalized Benzley's enriched element (Benzley, 1974). The fixed-free corner stress intensity factors are given and comparison of their computational results is presented.

KEYWORDS

Fracture singularity; numerical computation; singular finite element; fixed-free corner.

INTRODUCTION

It is well known that Williams solution (Williams, 1952) has been used as an asymptotic solution for boundary value problems with corners at fixed-free edges (Aksentian, 1967; Benthem & Minderhoud, 1972; Zak, 1964). Recently, his result has also been used for analyses of a V-notched plate and a strip with fixed-free corners (Lin & Tong, 1980; Stern & Soni, 1976; Nikooyeh & Robinson, 1981). Finite element approaches have been proposed for fracture mechanics problems where derivative singularity $O(r^{-1/2})$ exist. However, the nature of the problem addressed here is related to that of the classical fracture problem except that the boundary condition is mixed, that is, one side of the corner is subjected to a traction free and the other to a zero-displacement boundary condition. This type of singularity appears in the stress analysis of a layered medium under compression. It has implications in the fracture or failure analysis of the composites. Three approaches were used in studying the mixed problem. The first approach uses the regular bilinear isoparametric quadrilateral element (Zienkiewicz, 1977). The second uses Akin's special four-node quadrilateral element (Akin, 1976), and the third is based on a generalized Benzley's enriched element (Benzley, 1974).

In developing the techniques for solution, a slab with one end subject to a uniform pressure, and another end fixed, is chosen as an example (see Fig. 1). The fixed-free corner stress intensity factors may be determined indirectly or directly from the second approach and third approach and will be compared with an available solution (Stern & Soni, 1976; Gupta, 1975).

THE FIXED-FREE CORNER STRESS INTENSITY FACTORS

In the following we assume that the Williams' solution (Williams, 1952) is applicable to the analysis of the corner of a slab (or a strip). Consider a slab (or strip) with fixed-free corners as shown in Fig. 1. The boundary conditions are assumed to be

$$\theta = 0, \qquad u_r\big|_{\theta=0} = 0 \qquad u_\theta\big|_{\theta=0} = 0$$
$$\theta = \alpha, \qquad \sigma_\theta\big|_{\theta=\alpha} = 0 \qquad \tau_{r\theta}\big|_{\theta=\alpha} = 0 \tag{1}$$

where r, θ are the polar coordinates; u_r, u_θ are the displacement components and σ_θ, $\tau_{r\theta}$ are the stress components.

Using Williams' solution, through the transformation of coordinates, we obtain the stresses and displacements near the corner as follows:

$$\sigma_x = \lambda r^{\lambda-1}\{A[(4\sigma-1+\lambda)\cos(\lambda-1)\theta-(\lambda-1)\cos(\lambda-3)\theta]+C[(5-4\sigma+\lambda)\sin(\lambda-1)\theta -(\lambda-1)\sin(\lambda-3)\theta]\}$$

$$\sigma_y = \lambda r^{\lambda-1}\{A[(5-4\sigma-\lambda)\cos(\lambda-1)\theta+(\lambda-1)\cos(\lambda-3)\theta]+C[(4\sigma-1-\lambda)\sin(\lambda-1)\theta +(\lambda-1)\sin(\lambda-3)\theta]\}$$

$$\tau_{xy} = \lambda r^{\lambda-1}\{A[(3-4\sigma-\lambda)\sin(\lambda-1)\theta+(\lambda-1)\sin(\lambda-3)\theta]+C[(3-4\sigma+\lambda)\cos(\lambda-1)\theta -(\lambda-1)\cos(\lambda-3)\theta]\} \tag{2}$$

$$u = \frac{r^\lambda}{\mu}\{A(-\lambda\sin(\lambda-1)\theta\sin\theta)+C[(3-4\sigma)\sin\lambda\theta+\lambda\cos(\lambda-1)\theta\sin\theta]\}$$
$$v = \frac{r^\lambda}{\mu}\{A[3-4\sigma)\sin\lambda\theta-\lambda\cos(\lambda-1)\theta\sin\theta]+C(-\lambda\sin(\lambda-1)\theta\sin\theta)\} \tag{3}$$

where μ is the shear modulus; $\sigma = \nu$ for a plane strain problem, $\sigma = \nu/(1+\nu)$ for a plane stress problem where ν is the Poisson ratio and λ is the eigen-value of the following equation:

$$\sin^2\lambda\alpha = \frac{4(1-\sigma)^2}{3-4\sigma} - \frac{\sin^2\alpha}{3-4\sigma}\lambda^2 \tag{4}$$

In (2) and (3) A and C are undetermined coefficients. Equation (4) has a pair of real roots, other roots being complex. In this paper we chose only a positive real root and assumed that it is an adequate approximation.

The fixed-free corner stress intensity factors are defined as

$$K_I = \lim_{r\to0} r^{1-\lambda}\,\sigma_\theta\big|_{\theta=0} = \lim_{x\to0} x^{1-\lambda}\,\sigma_y\big|_{y=0}$$
$$K_{II} = \lim_{r\to0} r^{1-\lambda}\,\tau_{r\theta}\big|_{\theta=0} = \lim_{x\to0} x^{1-\lambda}\,\tau_{xy}\big|_{y=0} \tag{5}$$

and

$$K = \frac{K_{II}}{K_I} = \frac{C}{A} = \frac{\sin^2\alpha + \sin^2\lambda\alpha}{\cos^2\alpha - \cos^2\lambda\alpha - (3-4\sigma+\lambda)} \tag{6}$$

substituting (2) into (5), we obtain

$$K_I = 4(1-\sigma)\lambda\, A$$
$$K_{II} = 4(1-\sigma)\lambda\, C \tag{7}$$

which describe the singularities at the fixed-free corner.

ELEMENT FORMULATION

In the present paper, the type of elements used are (1) the regular bilinear isoparametric quadrilateral element (Zienkiewicz, 1977), (2) Akin's special four-node quadrilateral element (Akin, 1976), and (3) the generalized Benzley's enriched element (Benzley, 1974). Both (2) and (3) are combined with (1) in the methods of solution discussed hereafter. Some details of the elements are described below.

1) Regular Bilinear Isoparametric Quadrilateral Element

The displacements u_i are defined as (Fig. 2)

$$u_i = \sum_{k=1}^{4} f_k\,\bar{u}_{ik} \qquad (i = 1,2) \tag{8}$$

where f_k are shape functions given by

$$f_1 = \frac{1}{4}(1-\xi)(1-\eta)$$
$$f_2 = \frac{1}{4}(1+\xi)(1-\eta)$$
$$f_3 = \frac{1}{4}(1+\xi)(1+\eta)$$
$$f_4 = \frac{1}{4}(1-\xi)(1+\eta) \tag{9}$$

and $\bar{u}_{ik}$ are the nodal values of u_i.

2) Akin's Four-Node Special Element

To combine with the regular isoparametric element, we need to change the local coordinates s and t of Akin's element to the isoparametric coordinates ξ and η by the following expressions

$$s = \frac{1}{2}(1+\xi)$$
$$t = \frac{1}{2}(1+\eta) \tag{10}$$

Thus, the displacements in this element are assumed as (Fig. 2)

$$u_i = \sum_{k=1}^{4} N_k\,\bar{u}_{ik} \qquad (i = 1,2) \tag{11}$$

where N_k are the shape functions of the special element given by

$$N_k = \delta_{jk}(1 - \frac{1}{R}) + \frac{f_k}{R} \tag{12}$$

where $R = (1-f_j)^{1-\lambda}$, and j is the singular node number, others are not; δ_{jk} is the Kronecker delta. Here f_k are the same as in (9). λ is the constant given by (4) and related to the Poisson's ratio ν of the material of the element, and the angle between the fixed and free edges of the corner. In the development of this technique, we found that Akin's standard element is just the isoparametric bilinear quadrilateral element defined by (8). As was discussed by Akin, the element defined by (11) is compatible with those adjoining isoparametric elements defined by (9) and satisfies the following equations:

$$\sum_{k=1}^{4} N_k = 1, \qquad \sum_{k=1}^{4} \frac{\partial N_k}{\partial \xi} = 0, \qquad \sum_{k=1}^{4} \frac{\partial N_k}{\partial \eta} = 0. \tag{13}$$

For this element we use the following relations

$$x_i = \sum_{k=1}^{4} f_k \bar{x}_{ik} \qquad (i = 1,2) \tag{14}$$

to establish the coordinates transformation between the global coordinates and the isoparametric local coordinates, where $\bar{x}_{ik}$ are the nodal values of x_i.

3) Generalized Benzley's Enriched Element

Similar to the derivation of Benzley's enriched element, we define the displacements in the element as (see Fig. 2)

$$u_i = \sum_{k=1}^{4} f_k \bar{u}_{ik} + A[Q_i(r,\theta) - \sum_{k=1}^{4} f_k \bar{Q}_{ik}] \qquad (i = 1,2) \tag{15}$$

where f_k are the same as that in (9), and A is given in (2). $Q_i(r,\theta)$ derived from (3) gives the proper singularity at the corner. $\bar{Q}_{ik}$ are the nodal values of $Q_i(r,\theta)$. For the fixed-free corner,

$$Q_1(r,\theta) = g_1(\theta)r^{\lambda}, \qquad Q_2(r,\theta) = g_2(\theta)r^{\lambda} \tag{16}$$

where

$$g_1(\theta) = \frac{1}{\mu}[-\lambda\sin(\lambda-1)\theta\sin\theta + (3-4\sigma)K\sin\lambda\theta + \lambda K\cos(\lambda-1)\theta\sin\theta]$$

and

$$g_2(\theta) = \frac{1}{\mu}[-\lambda K\sin(\lambda-1)\theta\sin\theta + (3-4\sigma)\sin\lambda\theta - \lambda\cos(\lambda-1)\theta\sin\theta] \tag{17}$$

where K is a constant defined by (6) and λ is obtained from (4).

COMPARISON OF THE COMPUTATIONAL RESULTS

Using the foregoing three approaches, we analyzed a slab with the length to width ratio of 0.5. From the symmetry consideration, only one half of the slab was subjected to stress analysis and the same 64 element grid used in three approaches is shown in Fig. 3. Type A element designates the regular element in the first approach, the special element in the second and the enriched element in the third approach, respectively; other elements are the regular elements. When integration of the element stiffness matrix are performed, (3 x 3) and (7 x 7) Gauss quadrature were used for type A element in the second and third approach, respectively. The computational results of the normal and the shear stress distribution at the fixed edge and the displacement in the x-direction at the free edge by three approaches are shown in Figs. 4-6. It is observed that in the first approach we need refined meshes to obtain the stress distribution of a reasonable accuracy near the corner. The second approach gives results in the stress distribution very close to those given by G. P. Gupta (Gupta, 1975). This evidence lends support to Gupta's approach. The third approach provides directly an approximate value of the coefficient A. From (6) and (12) we can obtain an asymptotic stress distribution, as shown by the triangular points in Figs. 4 and 5, which lie below the results obtained from the second approach. Since this element has an additional term, it is incompatible with the adjoining standard elements. To improve the compatibility we used two types of transition elements to obtain (1) the displacement continuity and (2) both the displacement and the stress continuity at the interface of the adjoining elements. In both cases, the singularity exhibited by the computational results shows degeneracy ($|A| \ll 1$). Otherwise, the results are subjected to the effect of the size of the element, the larger the size the larger is the value of A.

From the numerical results of the stress by the second approach and using (6) and (7), we can indirectly calculate the fixed-free corner stress intensity factors. Table I shows some numerical results of the fixed-free corner stress intensity factor of the slab and the strip for two length-to-width ratios. For L/H = 0.5, 160 grid was used whereas for L/H = 0.25, 96 grid was used. The Poisson's ratio was 0.3. These results can be compared with Gupta's results which appeared in Stern and Soni (1976). A discrepancy of less than 5% was found. Notice that in Gupta's paper both ends were fixed, whereas in this paper the upper end is subjected to a uniform pressure. To compare results, L/H = 0.5 of this paper corresponds to L/H = 1.0 in Stern and Soni (1976).

TABLE I Fixed-Free Corner Stress Intensity Factor $K_I/Ph^{1-\lambda}$

$\frac{K_I}{Ph^{1-\lambda}}$	$\frac{L}{H} = 0.5$	$\frac{L}{H} = 0.25$
Slab	0.7879	0.7651
Strip	0.7636	0.7414

CONCLUSION

One way to describe the singularities of a fixed-free corner is to use the fixed-free corner stress intensity factors. The second approach described gives good results in the stress distribution and the fixed-free corner stress intensity factors. The method is general and easy to program. The third method, although used successfully in calculating the stress intensity factor for a crack, has obvious disadvantages: the element is incompatible with the adjoining standard elements. Also, observing from the comparison of stress distribution (Figs. 4-5) the accuracy of this approach appears to be insufficient.

REFERENCES

Akin, J. E. (1976). Int. J. Num. Method. Engng., Vol. 10, 1249-1259.

Aksentian, O. K. (1967). PMM, Vol. 31, No. 1, 178-186.

Benthem, J. P., and P. Minderhoud (1972). Int. J. Solids Structures, Vol. 8, 1027-1042.

Benzley, S. E. (1974). Int. J. Num. Meth. Engng., Vol. 8, 537-545.

Gupta, G. D. (1975). Journal of Applied Mechanics, Vol. 42, 81-87.

Lin, K. Y., and Pin Tong (1980). Int. J. Num. Meth. Engng., Vol. 15, 1343-1354.

Nikooyeh, H., and A. R. Robinson (1981). Int. J. Solids Structures, Vol. 17, 669-682.

Stern, M., and M. L. Soni (1976). Int. J. Solids Structures, Vol. 12, 331-337.

Williams, M. L. (1952). Journal of Applied Mechanics, Vol. 19, Trans. ASME, Vol. 74, 526.

Zak, A. R. (1964). J. of Applied Mechanics, Vol. 31, Trans. ASME, Vol. 86, 150-152.

Zienkiewicz, O. C. (1977). The finite element method, Third Edition, McGraw-Hill.

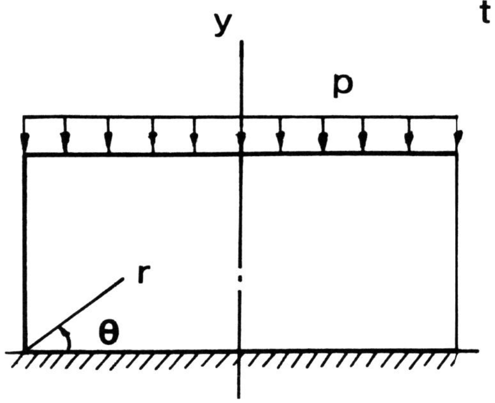

Fig.1 a slab

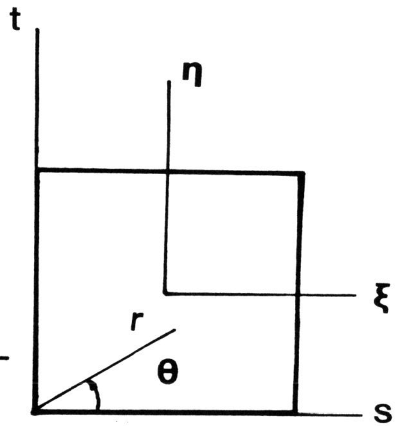

Fig.2 element

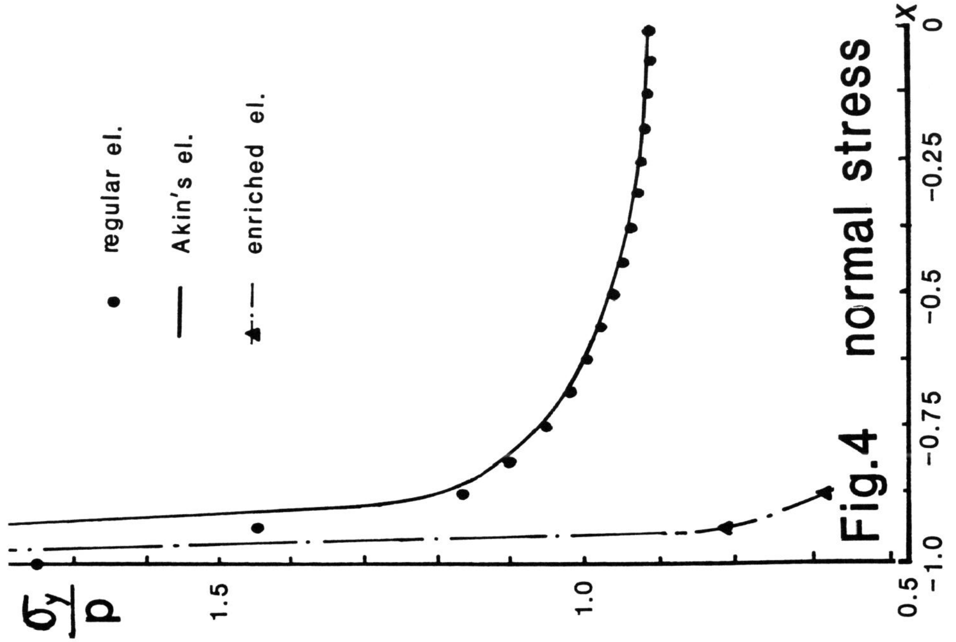

Fig.4 normal stress

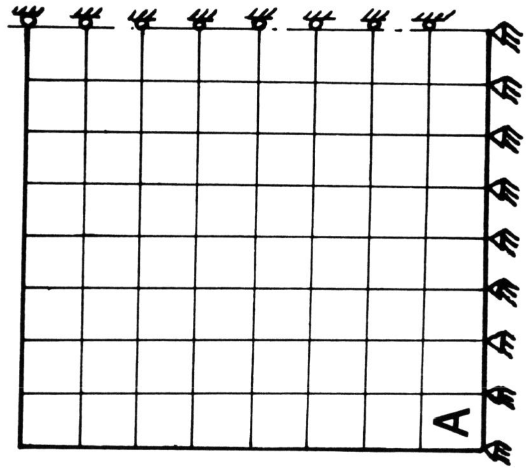

Fig.3 element meshes

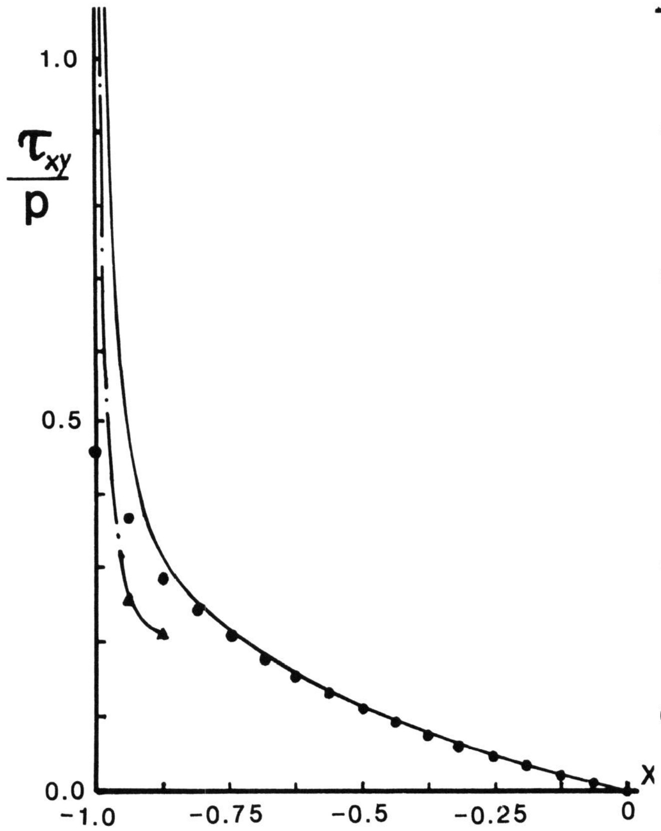

Fig.5 shear stress

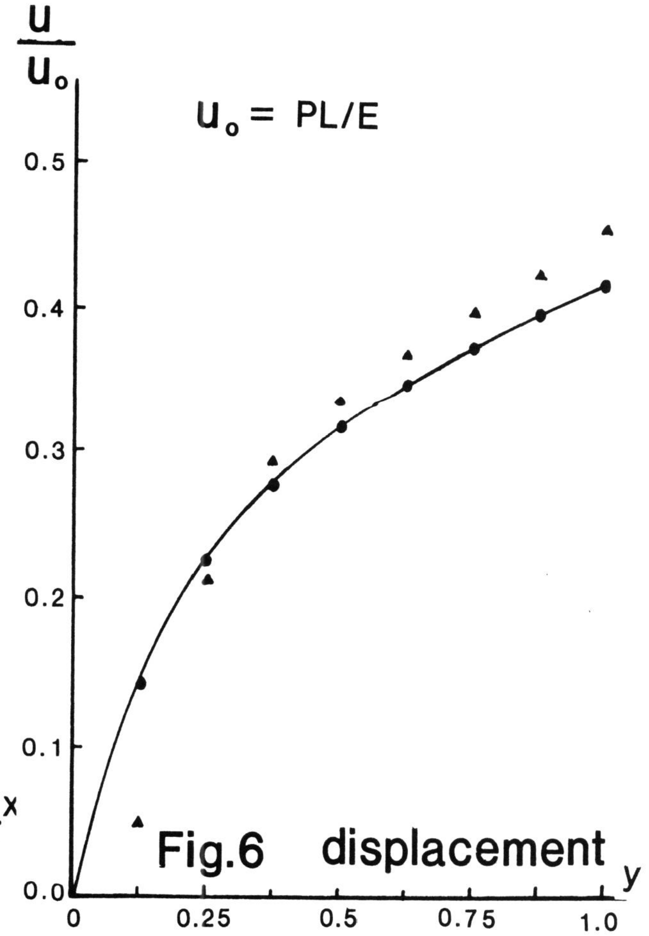

Fig.6 displacement